Concept of the solar-pumped laser-photovoltaics combined system and its application to laser beam power feeding to electric vehicles

Tomoyoshi Motohiro[1,2,3,4]*, Yasuhiko Takeda[3], Hiroshi Ito[1], Kazuo Hasegawa[3], Akio Ikesue[1], Tadashi Ichikawa[3], Kazuo Higuchi[1,3], Akihisa Ichiki[1,2], Shintaro Mizuno[3], Tadashi Ito[3], Noboru Yamada[3], Hom Nath Luitel[3], Tsutomu Kajino[3], Hidetaka Terazawa[2], Satoshi Takimoto[2], and Kemmei Watanabe[2]

[1]*Materials Science and Energy Engineering Division, Green Mobility Research Institute, Institutes of Innovation for Future Society, Nagoya University, Nagoya 464-8603, Japan*
[2]*Graduate School of Engineering, Nagoya University, Nagoya 464-8603, Japan*
[3]*Toyota Central R&D Labs., Inc., Nagakute, Aichi 480-1192, Japan*
[4] *Graduate School of Engineering, Toyota Technological Institute, Nagoya 468-8511, Japan*

*E-mail: motohiro@gvm.nagoya-u.ac.jp

We have developed a compact solar-pumped laser (μSPL) employing an off-axis parabolic mirror with an aperture of 76.2 mm diameter and an yttrium aluminum garnet (YAG) ceramic rod of φ1 mm×10 mm doped with 1% Nd and 0.1% Cr as a laser medium. The laser oscillation wavelength of 1.06 μm, just below the optical absorption edge of Si cells, is suitable for photoelectric conversion with minimal thermal loss. The concept of laser beam power feeding to an electric vehicle equipped with a photovoltaic panel on the roof was proposed by Ueda in 2010, in which the electricity generated by solar panels over the road is utilized to drive a semiconductor laser located on each traffic signal along the road. By substituting this solar-electricity-driven semiconductor laser with a solar-pumped laser, the energy loss of over 50% in converting the solar electricity to a laser beam can be eliminated. The overall feasibility of this system in an urban area such as Tokyo was investigated.

1. Introduction

Silicon photovoltaics (PV) has recently attained an energy conversion efficiency η as high as 25.6%[1),2)]. It will unquestionably play a major role in PV for some time in the future because of the abundance of Si natural resources. As early as 1996, the University of New South Wales in Australia attainedη =24.0%[3)]. From the measured data of spectral quantum efficiency published in Ref. 3, the spectral energy conversion efficiency η(λ) can be calculated as shown in Fig. 1, where λ stands for wavelength. η(λ) takes a maximum value of over 40% at λ just below the optical absorption band edge of Si of 1117 nm. The solar spectrum, which is also illustrated with its intensity in arbitrary unit for comparison, has a maximum at around 500 nm. Obviously, the solar spectrum does not make a good fit with η(λ). Over the range of wavelengths in Fig. 1, η for crystalline Si solar cells decreases to as low as 25-30%. The residual 70-75% of the solar energy contributes only to the temperature rise of the cell. In contrast, the lasing wavelength of a Nd:glass laser is located just below 1117 nm and closely fits to the peak of η(λ). This means that the photon energy can be converted to electricity with minimal heat loss. In addition to the Nd:glass laser, Nd-doped yttrium aluminum garnet (YAG) ceramic[4),5)] is also a good laser medium and yields a laser with a similar wavelength. By focusing sunlight, the Nd-doped YAG ceramic can be and yield a laser beam with a wavelength around the peak of η(λ). In this paper, the feasibility of combining this solar pumped laser (SPL) and PV is discussed with special attention to laser beam power feeding to an electric vehicle equipped with a photovoltaic panel on the roof.

2. Conventional SPL

The first SPL was reported by Young in 1966[6)], which was only 6 years after the first achievement of ruby laser oscillation by Maiman in 1960[7)]. Young's SPL employed a parabolic mirror of 61 cm caliber and Nd-doped glass as well as a Nd-doped YAG (Nd:YAG) crystal and oscillated at 1 W. More recently, in 2000 s, the successful fabrication of laser rods of transparent YAG ceramic of excellent optical quality intensified research and development (R&D) activities on SPLs. Yabe et al. attained SPL oscillation of 80 W at a sunlight-to-laser conversion efficiency of 4.3% by concentrating natural sunlight by a factor of 2500 onto the end of a laser rod of 10 mm diameter and 100mm

length using a 2×2 m^2 Fresnel lens. The laser beam output was focused onto MgO at an optical power density of 10^5 W/cm^2 to attain a temperature of 4000 K at which MgO is thermally decomposed to yield metallic Mg. The resultant metallic Mg was to be utilized in the "Mg-H_2 cycle", where the lightweight metallic Mg grains are transported as an energy carrier and H_2 is produced by pouring water onto the metallic Mg grains at the required location[8),9)]. The resultant MgO produced by the degeneration of water is then thermally decomposed again under the focused laser light from the SPL.

One of the technical problems to deal with is the inhomogeneous temperature rise of the laser medium under the illumination of focused sunlight because of the low thermal conductivity of Nd-doped glass and Nd:YAG ceramic. This may cause an inhomogeneous change in the refractive index of the medium, which leads to the cessation of lasing and even irreversible degradation. Therefore, a forced-water-cooling system is usually necessary to achieve continuous lasing. The large-scale collector optics such as a 2×2 m^2 Fresnel lens or a parabolic mirror of 2 m diameter has another technical difficulty in tracking the sun because of air resistance under strong wind. The latter problem can also lower the number of operating days per year in conventional concentrating photovoltaic systems.

3. Development of microscale SPL

We employed a fluoride optical fiber of 5 μm diameter and 10 m length slightly doped with Nd as a laser medium because its large aspect ratio enables the rapid dissipation of heat from its side surface via natural air cooling. In parallel, we also employed a rectangular column (rod) of Cr,Nd:YAG ceramic of 1 mm×1 mm×5 mm as another type of laser medium. The sunlight is concentrated onto the end surface of the optical fiber or the rectangular column (rod) by a factor of 10626, employing off-axis parabolic mirrors as shown in Fig. 2 for both the rectangular column (rod) and the 10 m-long fiber. Since these SPLs are compact and lightweight without any water-cooling system, they can be mounted on a commercially available solar-tracking system for an astrometric telescope as shown in Fig. 3[10)-12)]. In this paper, these SPLs are abbreviated as (μSPLs), hereafter.

Continuous lasing while tracking the sun was confirmed between 14:40 and 15:40 on a day in September. Lasing was also observed even at 16:00, indicating possible lasing hours between 8:00 and 16:00 as shown in Fig. 4.

4. Photoelectric conversion of monochromatic laser light from μSPL

The laser output is transmitted via an optical fiber to a room indoors at a distance of 100 m from the SPL with attenuation within 0.18 dB, where photoelectric conversion can be performed in two ways.

4.1 Photoelectric conversion under high optical power density

Since the optical fiber exit is no larger than 0.1 mm in diameter, the intimate attachment of a small photoelectric conversion device to the exit of the optical fiber realizes the almost normal incidence of the monochromatic light, which enables the almost ideal design of an antireflecting multilayered bandpass filter to minimize optical power loss. However, the optical power density of the incident laser can be as high as 800 W/cm^2 or more. The resultant extremely high photocurrent density can decrease the energy conversion efficiency because of the large resistive loss. To prevent this, a specially designed single-crystal Si photovoltaic cell, in which the optical absorption layer is as thin as 0.05 mm, was fabricated to reduce the resistive loss as schematically shown in Fig. 5. To enhance optical confinement in this thin optical absorption layer, diffuse reflection inside the absorption layer and band-pass filtering at the incidence of the laser beam are combined. The theoretical upper limit of the energy conversion efficiency of the incident laser is estimated to be as high as 61%. Experimentally, the energy conversion efficiency of 30% under the illumination of laser light with a wavelength of 1.06 μm and an optical power density of 22 W/cm^2 has thus far been confirmed[13)-16)].

Another possible means besides photovoltaic cells is an optical rectenna, which receives light as an electromagnetic wave via an optical antenna, and the received high-frequency alternate current is rectified by a high-frequency diode to yield electric power[17)]. The maximum energy conversion efficiency for monochromatic polarized laser light such as the output of a μSPL is expected to be more than 80%[18)]. The size of the optical rectenna is of the nm scale, corresponding to the wavelength of light. Therefore, nanoscale fabrication technology, which limits the area of the devices, is necessary. The cross section of the optical fiber is small enough for such nanofabrication technology.

The recent rapid progress in plasmonics will also be helpful for the development of optical rectennas.

4.2 Photoelectric conversion under low optical power density

To achieve photoelectric conversion at the end surface of the optical fiber output under a high optical density, it is necessary to develop specially designed photovoltaic cells or optical rectennas as described in Sect. 4.1. There is another way to achieve the photovoltaic conversion of the SPL output laser without using specially designed photovoltaic cells. As schematically indicated in Fig. 6, the laser light from a μSPL can be extracted gradually or in stepwise manner in the perpendicular direction of the optical fiber by mitigating the optical confinement condition. By introducing the resulting separated laser beams into an optical waveguide plate, as established in display technology, a monochromatic large-area light source with moderately diluted optical power density can be realized. By attaching a conventional Si solar panel designed for an incident optical power density of around 100 mW/cm^2 with the same area as the optical waveguide plate, a plate for a photoelectric conversion unit can be formed. By stacking plates of photoelectric conversion units, a "PV box" instead of a PV panel can be formed as indicated in Fig. 6. Since this PV box can be placed away from the μSPLs, such as in the soil or undersea, and because the temperature, humidity, and ambient gas composition in the PV box can be controlled on demand, the long-term stable generation of electricity may be realized even in a location where conventional solar panels cannot give a good performance. The minimal heat loss described in Sect. 1 also contributes to controlling the temperature. Because of the single-mode property of the μSPL output, the laser can be converted into that with a wavelength of 532 nm by frequency doubling using a nonlinear optical crystal with a conversion efficiency of nearly 80%. Therefore, in addition to the Si-based PVs, organic and organic-inorganic hybrid PVs can also be used for a long time in the controlled ambient[19),20)].

5. Cordinated solar tracking of an array of μSPLs

Advantages of the μSPL are its compactness and compatibility with mass production. To increase the output power, the coordinated solar tracking of an array of many μSPLs is

indispensable. Figure 7 shows a schematic of a coordinated solar tracking unit and an outdoor operating test on a roof terrace. Since we have found that laser emission from our μSPL can be sustained if the tracking error is within ±5 mrad, which is slightly more than half of the angular diameter of the sun, the coordinated solar tracking system is designed to keep the tracking error within 1 mrad. This coordinated tracking system has an advantage of its small perpendicular size, making it more durable against wind than an array on one panel[21)].

6. Improvement of energy conversion efficiency of μSPL

6.1 Improvement of spectral matching

The theoretical upper limit of the energy conversion efficiency of an SPL is around 48%, whereas the experimentally attained value is 2-3%. Figure 8 shows solar spectra with and without absorption during laser emission by the Nd,Cr:YAG laser rod in our μSPL system together with the laser emission spectrum. The optical power density of the absorbed portion of the spectrum is found to be as low as 30% of that of the portion without absorption. Although we found that 65-80% of the optical energy absorbed by Cr ions is transmitted to Nd ions and contributes to laser emission, it is necessary to find elements in addition to Cr to improve spectral matching[22)].

6.2 Improvement of mode matching

In the present μSPL employing a Cr,Nd:YAG laser rod, only 29% of excited Nd ions can contribute to laser emission since the other excited Nd ions are located outside of the mode matching region. This low mode matching ratio is connected to the present low energy conversion efficiency of the μSPL[23)]. To improve the ratio, the Nd and Cr ions located outside of the mode matching region should be eliminated. Figure 9 shows the cross-sectional and side views of a newly fabricated composite laser rod in which Nd and Cr ions are only doped in the green region near the central axis of the rod. The other region is doped with Gd ions to compensate for the refractive index difference. The photographs were taken before the completion of the polishing process to distinguish the clading-core interfaces. Experimental measurement accompanied by the computer simulation of the laser emission on this composite rod indicates that the energy conversion

efficiency can reach as high as 39% as a result of the improved mode matching.

7. Concept of laser beam power feeding from μSPLs to an electric vehicle equipped with a PV panel on the roof

7.1 Background to the concept

Recently, there has been rapid development in electric vehicles (EVs). To extend their range, attempts have been made to mount as many batteries as possible. To further extend the range, attempts have been made to mount a Si solar panel on the roof of some EVs. However, these tactics have a risk of adverse effects. Since the areal density of the energy flux of solar light is low, the energy gain due to the installation of a solar panel on the roof of an EV is limited. The PV panel must be reinforced to satisfy endurance tests for the roofs of automobiles, leading to an increase in the weight of the panel. Increasing the number of batteries and installing a PV panel on the roof also increase the weight of the vehicle, increasing fuel consumption and shortening the range. Ueda proposed the more efficient utilization of solar panels on the roof of EVs, where solar panels receive laser light from infrastructure along arterial roads[24]. The lasers along the road are operated using the electricity generated by solar panels also installed along arterial roads on the roofs of the roadside buildings, on arcades, and even on the roads themselves[25]. EVs should be installed with the minimal number of batteries to continue running in the intervals between the laser beam power feeding (hereafter, abbreviated as LBPF) and along branch roads where LBPF cannot be achieved. The PV panels should be as small as possible because of the limited cross section of the laser beam and targeted irradiation control. This has the merit of decreasing the weight of the vehicle and hence reducing energy consumption as shown in Fig. 10.

7.2 Case study for Tokyo city area

In the metropolitan area of Tokyo, the total area of the arterial roadways is 103 km^2, where the annual average insolation per unit area per day is 3.71 $kWh/m^2/day$[2 6]. Thus, the total insolation per day on all of Tokyo's roadways is 3.82×10^8 kWh/day. If PV panels of η=20% are employed, the total generated electricity will be 7.64×10^7 kWh/day. Using

this electricity, we suppose that semiconductor laser beams of 3.82×10^7 kWh/day can be pumped with an energy efficiency of 50%. Further more, we suppose that these monochromatic semiconductor laser beams can be converted to electricity at an energy conversion efficiency of 50% on a modest scale[13)-16)]. This means that 1.91×10^7 kWh/day can be utilized to run automobiles. Conservatively supposing the electricity consumption of a typical minivan EV to be 5 km/kWh[27)], then the electricity of 1.91×10^7 kWh/day can run minivan EVs for 9.6×10^7 km/day, or 9.6×10^7 vehicles· km/day. During the daytime, the majority of vehicles running in Tokyo metropolitan area are those for public transportation such as taxis and buses as well as for cargo transport including door-to-door deliveries. Since 2010, these vehicles have run 8×10^7 vehicles· km/day[28)] because of the saturation of traffic in Tokyo metropolitan area. This reveals that all these vehicles running in Tokyo metropolitan area can run by LBPF from solar power stations without using fossil fuel. In Japan, half of the energy consumption is for transportation. Therefore, the above scheme would make a major contribution to reducing CO_2 emission. It should also be noted that these vehicles could operate with much fewer batteries than present EVs. This means that the typical electricity consumption would be much less than 5 km/kWh and that the above scheme could run much more than 9.6×10^7 vehicles· km/day. In the scheme mentioned above, the energy conversion efficiency from solar electricity to laser was assumed to be smaller than 50%. If SPLs are used in this scheme, this 50% loss of energy can be eliminated and the EVs in Tokyo metropolitan area could run for twice the estimated value above, that is, 1.9×10^8 vehicles· km/day.

8. Discussion

SPL-driven vehicles were proposed by Yabe[29)], but not via photoelectric energy conversion but via direct propulsion by the laser ablation of a target on the vehicle based on the principle of action and reaction[30),31)]. Laser-driven vehicles via photoelectric energy conversion were first investigated in aerospace technology for application to lunar rovers[32)-35)]. Later, future laser-powered solar-electric unmanned aircraft and spacecraft were investigated by precisely beaming laser light to aircraft[36)-38)], so that they could be flown at night or at high latitudes during winter when days are short and nights are long.

More recently, terrestrial applications such as helicopters for data collection in the case of disasters have been investigated[39)-41)].

Here, the requisite of high accuracy of solar tracking owing to the high concentration ratio of sunlight may result in limited operation time. It is important to make SPLs work even in the case of weak direct insolation utilizing indirect insolation as in the case of PV cells. It is encouraging news that solar-pumped fiber lasers, that can operate without concentration of sunlight are being developed by Endo and Bisson.[42),43)]. They have proposed a solar-pumped fiber laser combined with a "greenhouse chamber" containing a liquid sensitizer in which an active fiber is immersed. The incident sunlight absorbed by the sensitizer is converted to the absorption band of the Nd ions in the fiber. According to their theoretical investigation, laser oscillation without the concentration of sunlight is feasible. On the basis of the above proposal of Ueda, the combination of SPLs and photoelectric conversion is expected to find new applications in mature cities such as Tokyo and Singapore in the near future.

The prospect for the fundamental durability of the system is next briefly mentioned. Although the excitation of Si with the optical adsorption edge at 1.1 eV by the monochromatic light of 1.06 μm (1.16 eV) minimizes the thermal loss, there will be a certain amount of thermal deposit in the PV cell in the case of the direct irradiation of the maximal SPL output. Thus, simulations of thermal diffusion were performed. The results indicate that the largest temperature increase due to illumination is 4°C. This is an acceptable value for ensuring durability. The durability of the optical fibers connecting the SPLs outdoors and the PV boxes under controlled circumstances is conjectured to be as follows. The durability of electrical power cables is specified as 15-20 years for outdoor use and 20-30 years for indoor use by Japanese Industrial Standards. The durability of optical fiber cables seems to be similar. Typical examples are 15 years for aerial cables and 21 years for underground cables (NTT West). For solid-state lasers, the working life is determined by the working life of the excitation light source. The typical lifetime is 1000 h for flash lamps or diode lasers. For SPLs, the working lifetime of the excitation light source is 5 billion years, the life of the sun. For the precision coordinated sun-tracking system for the group of SPLs shown in Fig. 7, some encapsulation for each group of SPLs will be necessary to protect sliding surfaces for long-term use.

9. Conclusions

The merits and challenges of solar photovoltaics via the photoelectric conversion of a monochromatic light from compact solar-pumped lasers (μSPLs) were investigated. Although the μSPL is still in the early stage of development, its possible energy conversion efficiency of 39% and the possible monochromatic conversion efficiency of a specially designed crystalline Si solar cell of 61% can result in a total energy conversion efficiency of 24%, which is comparable to the practical conversion efficiency of solar panels.

Utilizing such SPLs and PV in a combined system, the concept of LBPF to an electric vehicle equipped with a PV panel on the roof proposed by Ueda in 2010[24)] was re-evaluated. In this concept, the electricity generated by solar panels over a road is utilized to drive a semiconductor laser located on each traffic signal along the road. By substituting this solar-electricity-driven semiconductor laser with a solar-pumped laser, the energy loss of over 50% in converting the solar electricity to a laser beam can be eliminated. The overall feasibility of this system in urban areas such as Tokyo was investigated. In conjunction with the development of SPLs without the concentration of sunlight, the combination of SPLs and PV is expected to find new applications in LBPF to EVs with a small PV panel and the minimal number of secondary batteries in the near future.

Acknowledgment

This work was partially supported by the Advanced Low Carbon Technology R&D Program (ALCA) under Japan Science and Technology Agency.

References

1) M. A. Green, K. Emery, Y. Hishikawa, W. Warta, and E. D. Dunlop, Progress in Photovoltaics: Research and Applications **24**, 905 (2016).
2) http://www.nrel.gov/ncpv/images/efficiency_chart.jpg
3) J. Zhao, A. Wang, P. P. Altermatt, S. R. Wenham, and M. A. Green, Sol. Energy Mater. Sol. Cells **41-42**, 87 (1996).
4) A. Ikesue and Y. L. Aung, Nat. Photonics **2**, 721(2008).
5) A. Ikesue, Y. L. Aung, and V. Lupei, *Ceramic Lasers* (Cambridge University Press, New York, 2013), p. 121.
6) C. G. Young, Appl. Opt. **5**, 993 (1966).
7) T. H. Maiman, Nature **187**, 493 (1960).
8) T. Yabe, B. Bagheri, T. Ohkubo, S. Uchida, K. Yoshida, T. Funatsu, T. Oishi, K. Daito, M. Ishioka, N. Yasunaga, Y. Sato, C. Baasandash, Y. Okamoto, and K. Yanagitani, J. Appl. Phys. **104**, 083104 (2008).
9) T. Yabe, T. Ohkubo, S. Uchida, K. Yoshida, M. Nakatsuka, T. Funatsu, A. Mabuti, A. Oyama, K. Kakagawa, T. Oishi, K. Daito, B. Behgol, Y. Nakayama, M. Yoshida, S. Motokoshi, Y. Sato, and C. Baasandash, Appl. Phys. Lett. **90**, 261120 (2007).
10) H. Ito, K. Hasegawa, S. Mizuno, and T. Motohiro, Proc. 1st Advanced Lasers and Photon Sources Conf., 2012, p. 2.
11) S. Mizuno, H. Ito, K. Hasegawa, T. Suzuki, and Y. Ohishi, Opt. Express **20**, 5891 (2012).
12) S. Mizuno, K. Hasegawa, T. Ichikawa, H. Ito, T. Motohiro, T. Suzuki, and Y. Ohishi, 6th World Conf. Photovoltaic Energy Conversion Tech. Dig., 2014, p. 29.
13) Y. Takeda, H. Iizuka, S. Mizuno, K. Hasegawa, T. Ichikawa, H. Ito, T. Kajino, A. Ichiki, and T. Motohiro, J. Appl. Phys. **116**, 124506 (2014).
14) Y. Takeda, H. Iizuka, S. Mizuno, K. Hasegawa, T. Ichikawa, H. Ito, T. Kajino, A. Ichiki, and T. Motohiro, J. Appl. Phys. **116**, 014501 (2014).
15) Y. Takeda, H. Iizuka, T. Ito, S. Mizuno, K. Hasegawa, T. Ichikawa, H. Ito, T. Kajino, K. Higuchi, A. Ichiki, and T. Motohiro, Jpn. J. Appl. Phys. **54**, 08KA05 (2015).
16) Y. Takeda and T. Ito, Jpn. J. Appl. Phys. **54**, 08KD13 (2015).
17) *Rectenna Solar Cells* ed. G. Moddel and S. Grover, (Springer, New York 2013), p. 3.
18) M. A. Green, *Third Generation Photovoltaics* (Springer, Heidelberg, 2003) *Springer Series in Photonics*, Vol. 12, p. 21.
19) S. Takimoto, H. Ito, H. Terazawa, K. Watanabe, A. Ichiki, K. Higuchi, Y. Takeda, and T. Motohiro, presented at 26th Int. Photovoltaic Science and Engineering Conf. (PVSEC-26), 2016.
20) K. Watanabe, H. Ito, H. Terazawa, S. Takimoto, A. Ichiki, K. Higuchi, Y. Takeda, and T. Motohiro, presented at 26th Int. Photovoltaic Science and Engineering Conf. (PVSEC-26), 2016.
21) T. Motohiro, A. Ichiki, T. Ichikawa, H. Ito, K. Hasegawa, S. Mizuno, T. Ito, T. Kajino, Y. Takeda, and K. Higuchi, Jpn. J. Appl. Phys. **54**, 08KE04 (2015).
22) K. Hasegawa, T. Ichikawa, S. Mizuno, Y. Takeda, H. Ito, A. Ikesue, T. Motohiro, and M. Yamaga: Opt. Express **23**, A519 (2015).
23) H. Terazawa, H. Ito, K. Hasegawa, T. Ichikawa, A. Ichiki, and T. Motohiro, presented 26th Int. Photovoltaic Science and Engineering Conf. (PVSEC-26), 2016.
24) K. Ueda, DENKI-TSUSHIN-DAIGAKU-KIYO, **22**, 63 (2010) [in Japanese].

25) https://www.theguardian.com/environment/2016/dec/22/solar-panel-road-tourouvre-au-perche-normandy?CMP=Share_iOSApp_Other
26) http://app0.infoc.nedo.go.jp/metpv/monsola.html [in Japanese]
27) http://www.nissan.co.jp/ENV200/range.html [in Japanese].
28) https://www.kankyo.metro.tokyo.jp/climate/management/tokyo/circumstances.html [in Japanese].
29) T. Yabe, Proc. 3rd Int. Symp. Beamed Energy Propulsion (ISBEP3), 2004.
30) T. Yabe, C. Phipps, M. Yamaguchi, R. Nakagawa, K. Aoki, H. Mine, Y. Ogata, C. Baasandash, M. Nakagawa, E. Fujiwara, K. Yoshida, A. Nishiguchi, and I. Kajiwara, Appl. Phys. Lett. **80**, 4316 (2002).
31) T. Yabe, C. Phipps, K. Aoki, M. Yamaguchi, R. Nakagawa, C. Baasandash, Y. Ogata, M. Shiho, G. Inoue, M. Onda, K. Horioka, I. Kajiwara, and K. Yoshida, Appl. Phys. A **77**, 243 (2003) [in Japanese].
32) K. Takeda and N. Kawashima, Nihon Koku Uchu Gakkai Ronbunshi **51**, 393 (2003).
33) N. Kawashima and T. Takeda, Suppl. Adv. Astron. Sci. **108**, 291 (2003).
34) K. Takeda and N. Kawashima, Uchu Gijutsu **3**, 45 (2004) [in Japanese].
35) K. Takeda, N. Kawashima, and K. Yabe, Uchu Gijutsu **7**, 27 (2008) [in Japanese].
36) D. Bushman, Proc. Int. Workshop Laser Energy Transmission for Space Exploration and Ground Applications, 2004, p. 20.
37) D. Wake, J. Lightwave Technol. **26**, 2484 (2008).
38) http://www.nasa.gov/centers/dryden/history/pastprojects/Beam/index.html
39) K. Takeda and N. Kawashima, Koku Uchu Gijutsu **11**, 27 (2012) [in Japanese].
40) T. Nikitina, Proc. 28th European Photovoltaic Solar Energy Conf. Exhib, 2013, p. 544.
41) J. Sato, Proc. 10th Conf. Lasers and Electro-Optics Pacific Rim/18th OptoElectronics and Communications Conf./Photonics in Switching 2013, TuPO-8.
42) M. Endo and J. -F. Bisson, Jpn. J. Appl. Phys. **51**, 022701 (2012).
43) M. Endo, Kogaku 42, 466 (2013) [in Japanese].

Figure Captions

Fig. 1. (Color online) Spectral conversion efficiency of a crystalline Si solar cell[3)] under the monochromatic illumination of around 50 mW/cm^2. The solar spectrum is also illustrated. The lasing wavelength of the Nd:glass laser is indicated by an arrow.

Fig. 2. (Color online) Schematic diagrams of two different types ofμSPL: (a) fiber laser (core dia.: 5μm / inner cladding dia.: 125 μm / outer cladding dia.: 200 μm, length: 10 m, material: Nd 0.5%:ZBLAN (ZrF_4-BaF_2-LaF_3-AlF_3-NaF) glass) and (b) transparent ceramic rod laser (Cr, Nd-doped YAG, 1 mm×1 mm×5 mm).

Fig. 3. (Color online) Compact SPL on the solar tracking system for (a) fiber laser medium, (b) laser rod, and (c) rod-type laser medium.

Fig. 4. (Color online) Possible daytime lasing hours extrapolated from the corrected continuous lasing data from 14:40 to 15:40.

Fig. 5. (Color online) Specially designed single-crystal Si photovoltaic cell for normal-incident monochromatic laser light with a small beam diameter and high optical power density.

Fig. 6. (Color online) Photoelectric conversion under diluted optical power density.

Fig. 7. (Color online) Schematic of a coordinated solar tracking unit for an array of 25 μSPLs and a photograph of an outdoor operating test.

Fig. **8. (Color online)** Absorption and laser emission spectrum of μSPL: (a) absorption of solar spectrum by the laser rod and (b) laser emission spectrum.

Fig. **9. (Color online)** Clading-core-structured composite laser rod (clading: Gd-doped, core: Nd,Cr-codoped YAG).

Fig. **10. (Color online)** (a) Present trend of attempting to mount as many batteries as possible and a Si solar panel as large as possible on the roof of EVs to extend the range. (b) Future EVs combined with the infrastructure for LBPF. EVs should be installed with the minimal number of batteries to continue running in the intervals between LBPF, and along branch roads where LBPF cannot be achieved. The PV panels can be small because of the limited cross section of the laser beam and targeted irradiation control.

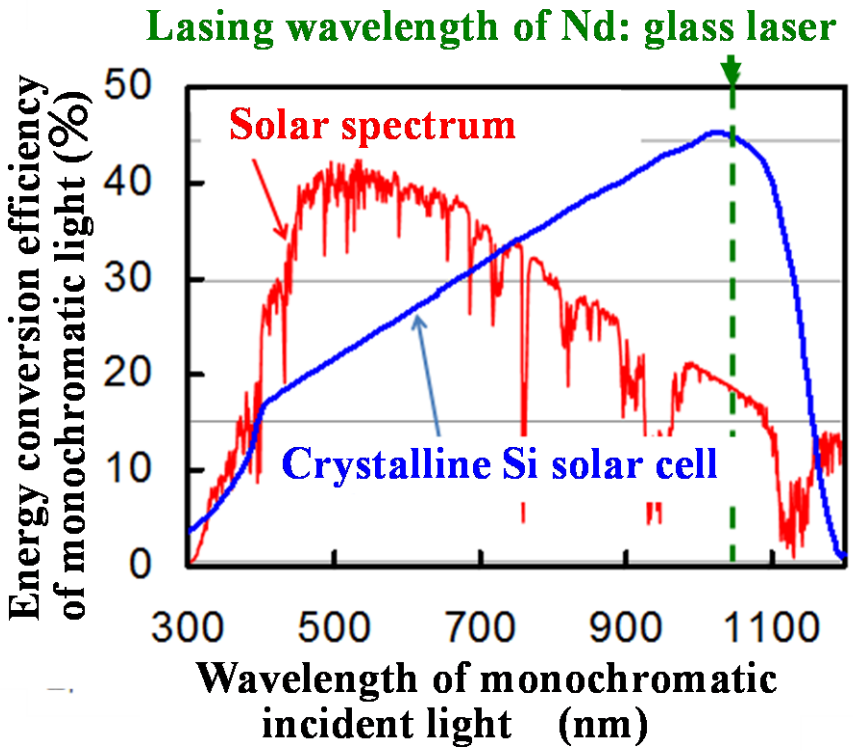

Fig.1. (Color Online)

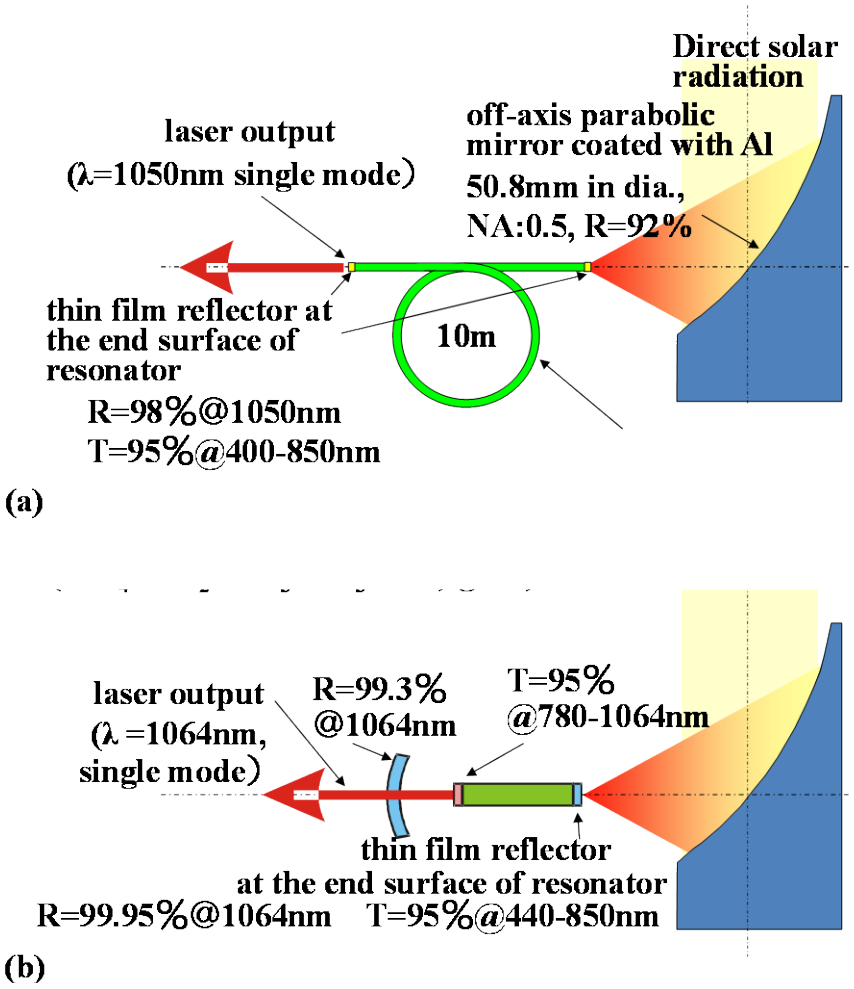

Fig. 2. (Color Online)

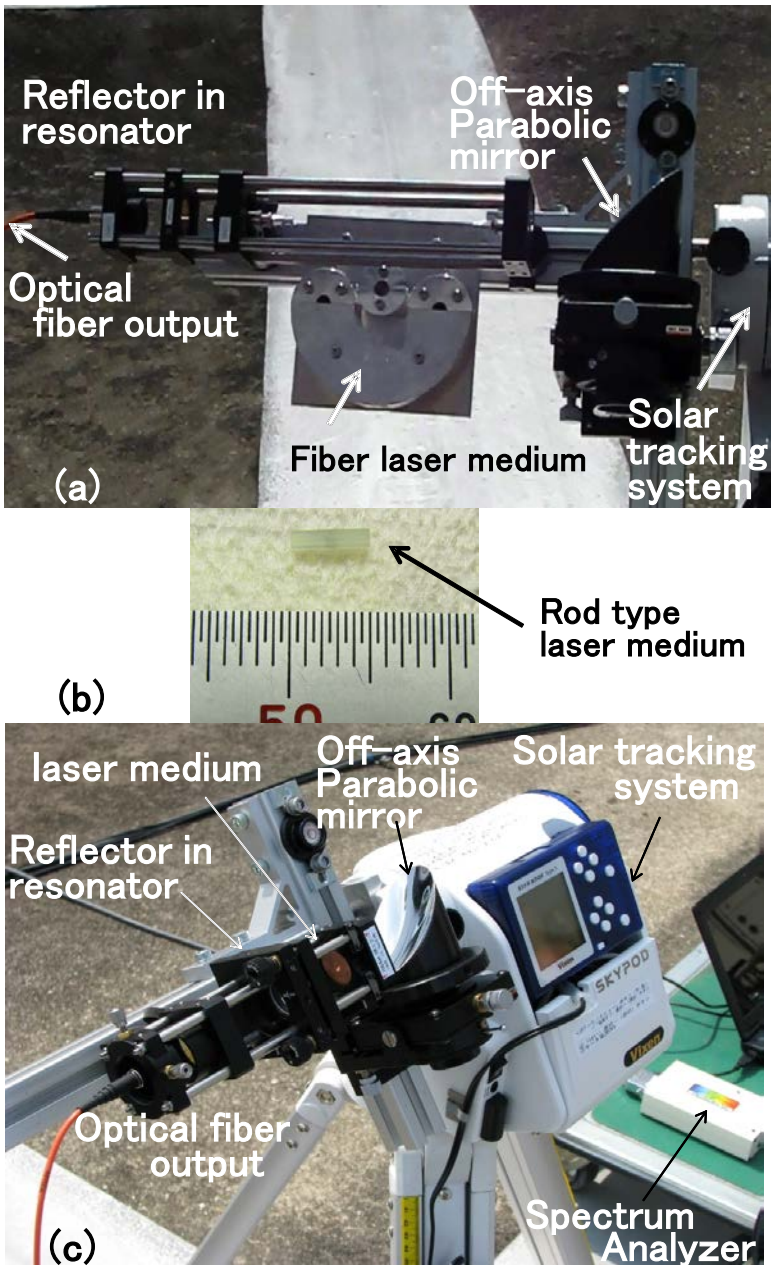

Fig.3 (Color Online)

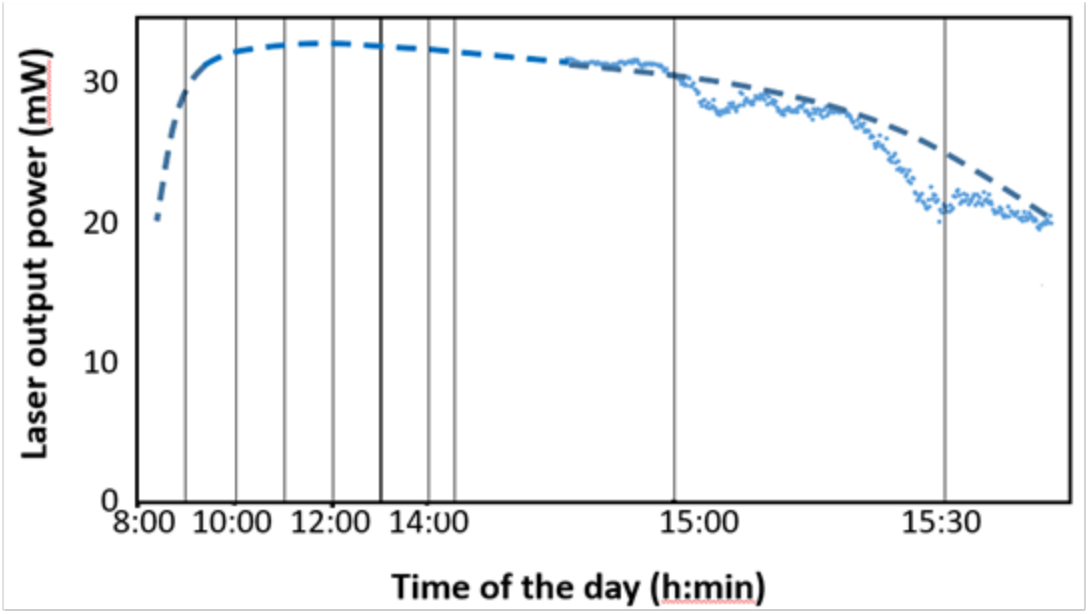

Fig.4 (Color Online)

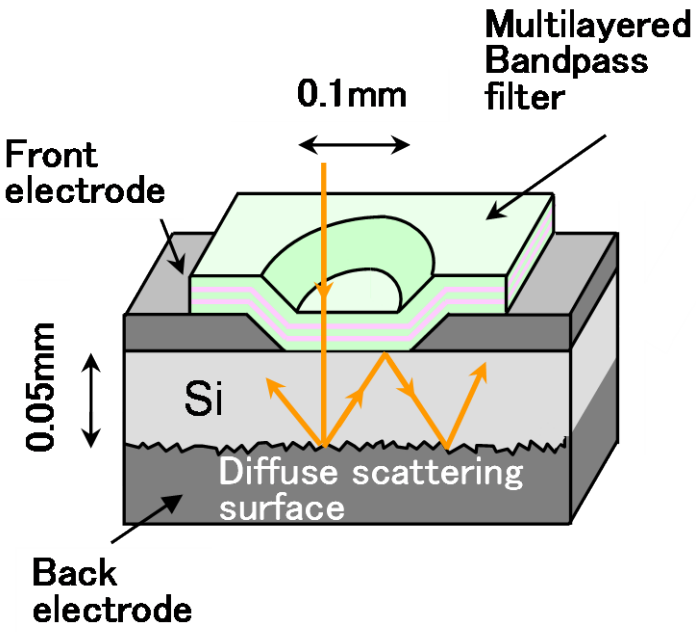

Fig.5 (Color Online)

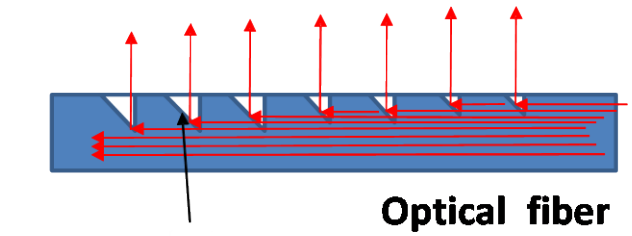

V-shaped groove for branching the laser light out of fiber

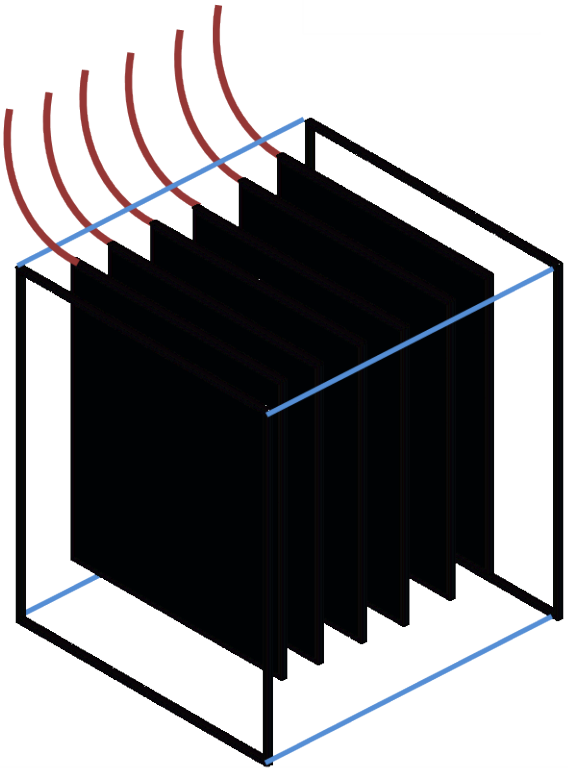

A stack pf plates of photoelectric Conversion unit under controlled Ciecumstances: “PV box”.

Fig.6 (Color Online)

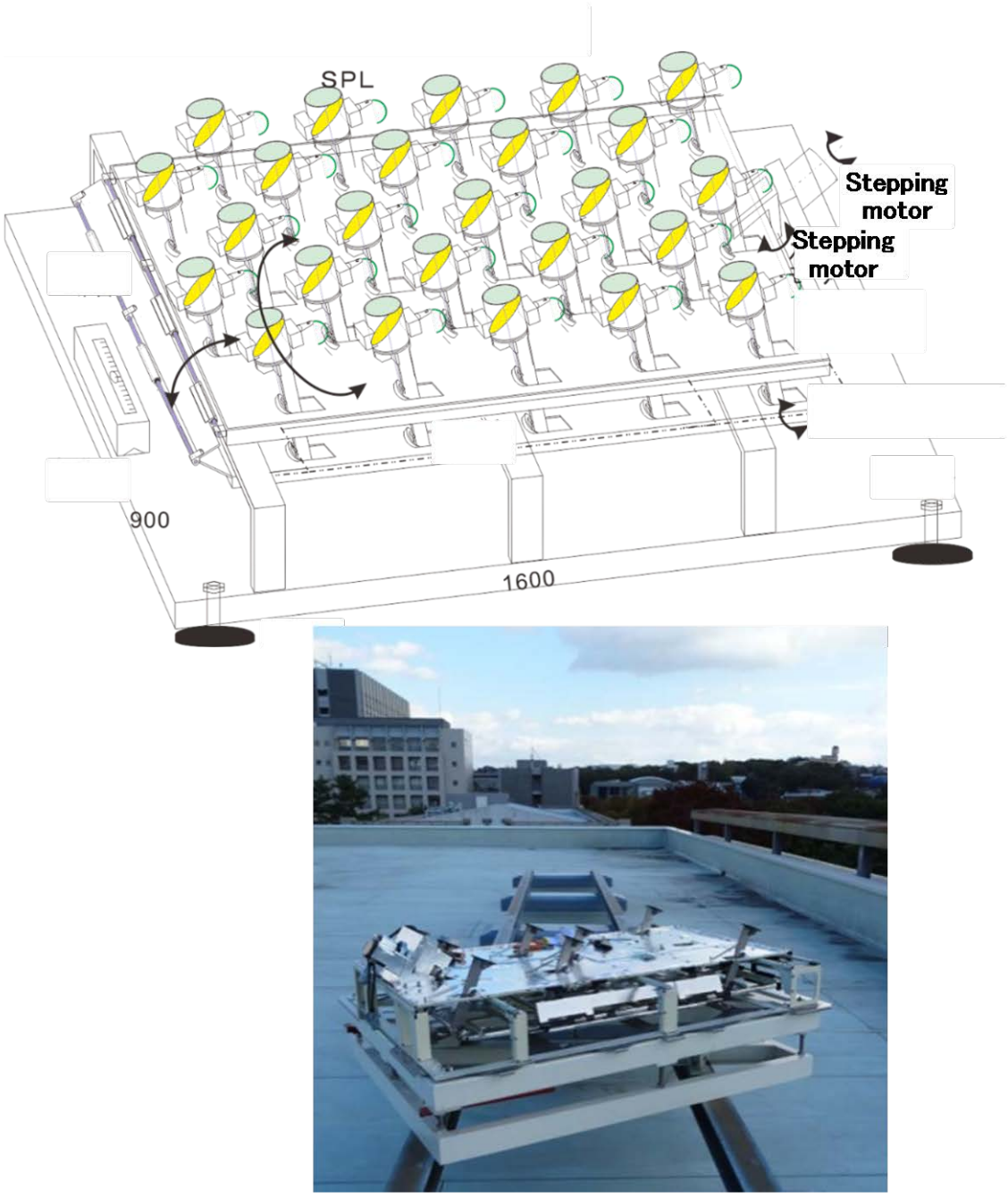

Fig.7 (Color Online)

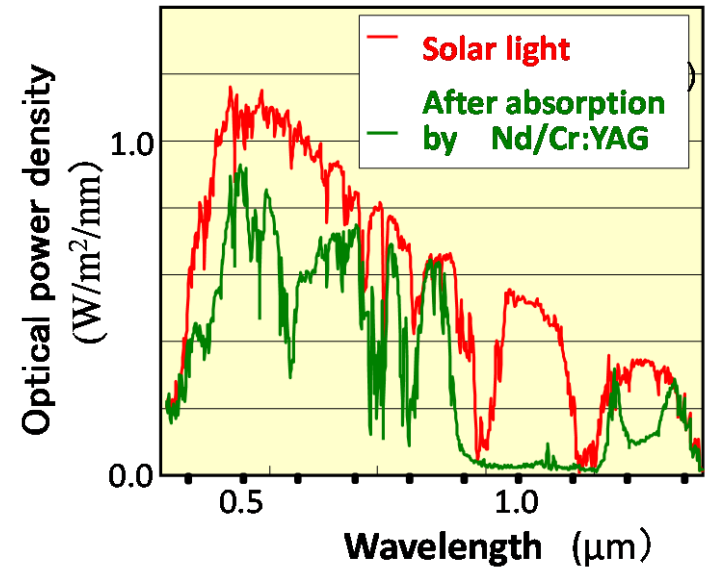

(a)

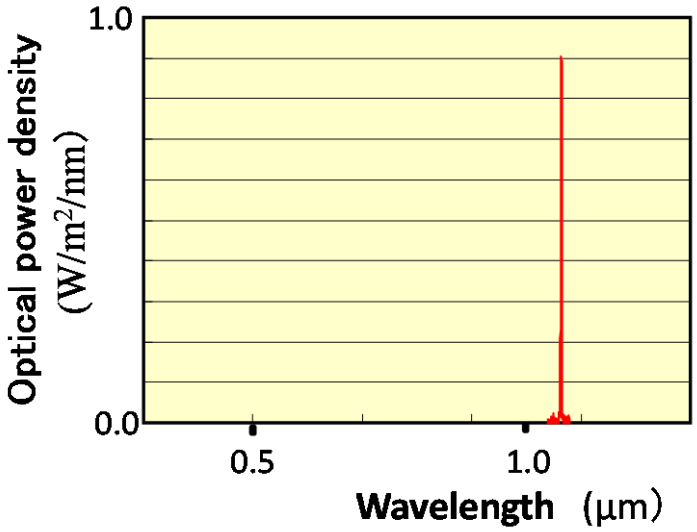

(b)

Fig.8 (Color Online)

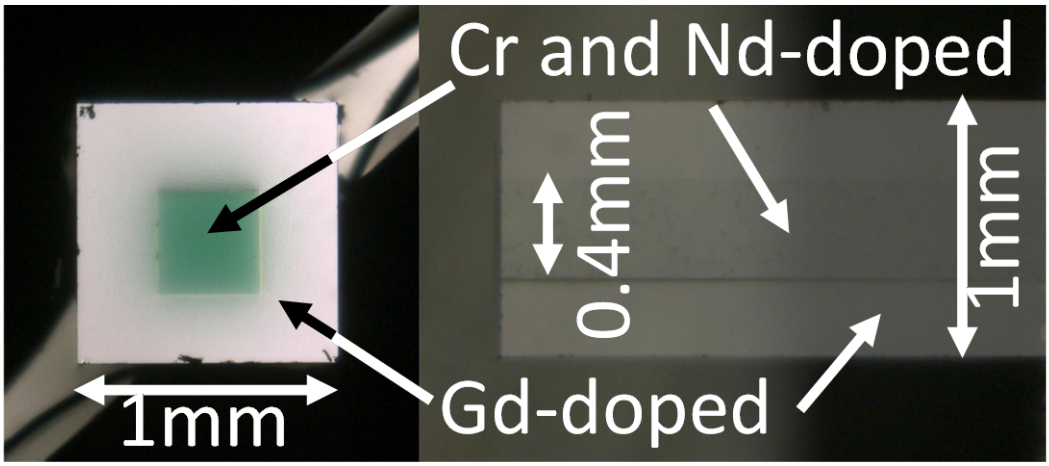

Fig.9 (Color Online)

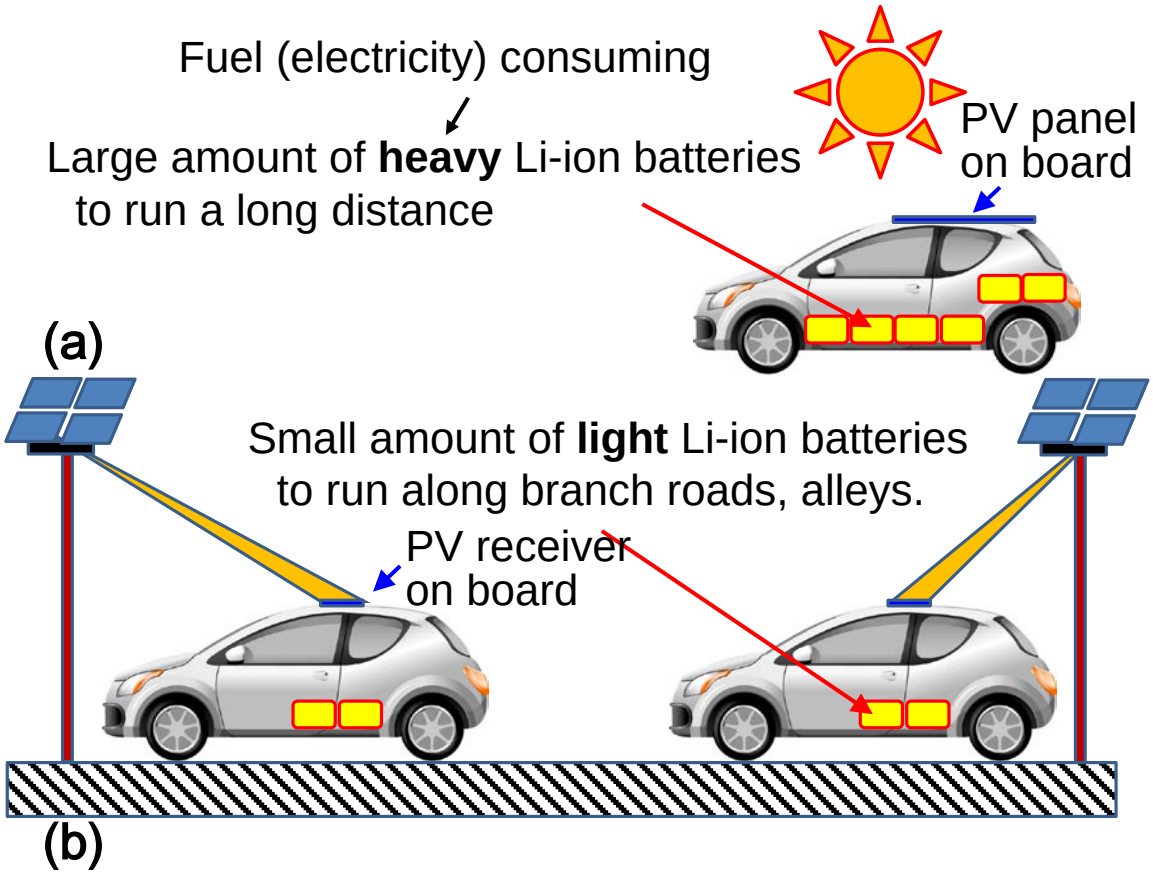

Fig.10 (Color Online)